Integrated Ferroelectrics
An International Journal

ISSN: (Print) (Online) Journal homepage: https://www.tandfonline.com/loi/ginf20

Ferroelectric Based Multi-Type Energy-Harvesting Device to Power a Mobile Medical Telemetry System

Alexander Molnar, David Gal, Henrietta Ban & Vitaly Gerasimov

To cite this article: Alexander Molnar, David Gal, Henrietta Ban & Vitaly Gerasimov (2021) Ferroelectric Based Multi-Type Energy-Harvesting Device to Power a Mobile Medical Telemetry System, Integrated Ferroelectrics, 220:1, 110-119, DOI: 10.1080/10584587.2021.1921540

To link to this article: https://doi.org/10.1080/10584587.2021.1921540

Published online: 01 Dec 2021.

INTEGRATED FERROELECTRICS
2021, VOL. 220, 110–119
https://doi.org/10.1080/10584587.2021.1921540

Taylor & Francis
Taylor & Francis Group

Ferroelectric Based Multi-Type Energy-Harvesting Device to Power a Mobile Medical Telemetry System

Alexander Molnar[a], David Gal[a], Henrietta Ban[a], and Vitaly Gerasimov[b]

[a]Department of the Physics of Semiconductors, Uzhhorod National University, Uzhhorod, Ukraine;
[b]Department of Light Industry, Mukachevo State University, Mukachevo, Ukraine

ABSTRACT

We have presented a multi-type energy-harvesting device for converting lighting, heating, and deformation to electricity using a composite material based on $Sn_2P_2S_6$ ferroelectric semiconductor to power the mobile medical telemetry equipment. To convert vibrations and motion, a second transducer layer is used, which is based on the triboelectric effect. It also uses $Sn_2P_2S_6$ powder as an active substance. Ferroelectric powder allows us to accumulate charge due to both the triboelectric and piezoelectric effect which significantly increases the efficiency of the converter. We have determined the pyroelectric, piezoelectric and photoelectric parameters of the composite active layer and triboelectric response amplitude and effectivity of triboelectric stage.

ARTICLE HISTORY
Received 23 November 2020
Accepted 25 March 2021

KEYWORDS
Ferroelectric; energy harvesting; triboelectric nanogenerator; photovoltaic effect

1. Introduction

Recently, interest in the medical, industrial, and commercial Internet of Things has increased significantly. For the energy supply of such equipment, it is advisable to use the energy of human movement, sunlight, temperature changes, and other phenomena, which allow us to create systems with almost unlimited working time. This task is especially relevant for employees of rescue services, who can perform their work for days without the possibility of recharging the equipment used (for example, when extinguishing forest fires). Today, there is a large number of devices that convert the energy of motion (due to the piezoelectric effect), lighting (due to the photovoltaic effect), or temperature changes in electricity. However, their use is subject to certain restrictions. Photoelectric converters cannot be used in the dark, motion converters in a static position, a pyroelectric converter with no temperature change. Therefore, it is very important to develop combined energy converters that can use several effects simultaneously. We have developed a flexible system for converting motion, lighting, and temperature changes into electrics using a composite material based on a $Sn_2P_2S_6$ ferroelectric powder.

Ferroelectrics are generally very promising materials for alternative micro energy. They simultaneously have piezoelectric, pyroelectric, and photovoltaic properties (Figure 1.). For example, a perovskite oxide solid-solution (1-x)$KNbO_3$-x$BaNi_{1/2}Nb_{1/}$

CONTACT Alexander Molnar alex.molnar@uzhnu.edu.ua

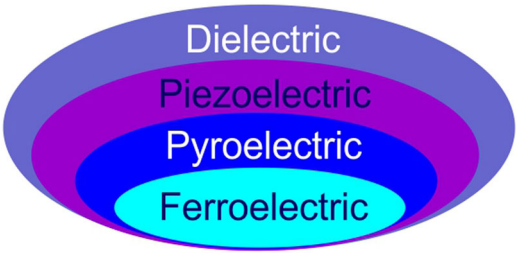

Figure 1. Piezoelectric, pyroelectric, and ferroelectric material relationships.

$_2O_{3-\delta}$ (KBNNO) is applicable for the development of hybrid energy harvesters/sensors, which can convert multiple energy sources into electrical energy simultaneously in the same material [1]. Most ferroelectric crystals are suitable for such an application. The main requirement for the candidates is the high value of the named coefficients and extended range of operating temperatures. One of the possible materials is $Sn_2P_2S_6$ and composites based on them [2].

In $Sn_2P_2S_6$ crystals, the second-order phase transition from the paraelectric phase ($P2_1/n$) to the ferroelectric phase (Pn) occurs at $T_c \approx 338$ K. At room temperature, spontaneous polarization is oriented in the (010) monoclinic symmetry plane near the [100] direction [3]. This type of crystal is photosensitive and wide energy bandgap ferroelectric semiconductors. In the ferroelectric phase, they exhibit a very strong piezoelectric effect. In pure $Sn_2P_2S_6$ single crystals the electromechanical coupling coefficient K_{11}=0.7 which is important for applications in alternate energy devices.

2. Energy Harvesting

2.1. Piezoelectric Effect

The mechanical energy such as stress or strain can be converted into electrical energy by the piezoelectric effect (Figure 2a). This strain can come from many different sources that exist everywhere, such as vibrations, body motion, and acoustic noise. When mechanical stress is applied to a piezoelectric sample, the crystal structure of the material is deformed, and this causes the movement of electrical charges [4].

2.2. Triboelectric Effect

The triboelectric nanogenerators, based on the contact electrification effect, provide a new approach to generating electricity from mechanical energy to operate small electronic devices. In the contact electrification effect, a material surface becomes electrically charged after it comes into contact with a different material through friction. This is the result of charge transfer between the two materials (Figure 2b) [5].

2.3. Photovoltaic Effect

Photovoltaic effect (PV) can convert light to usable electricity by using the PV effect [6], which is related to both the chemical and physical phenomena in the materials

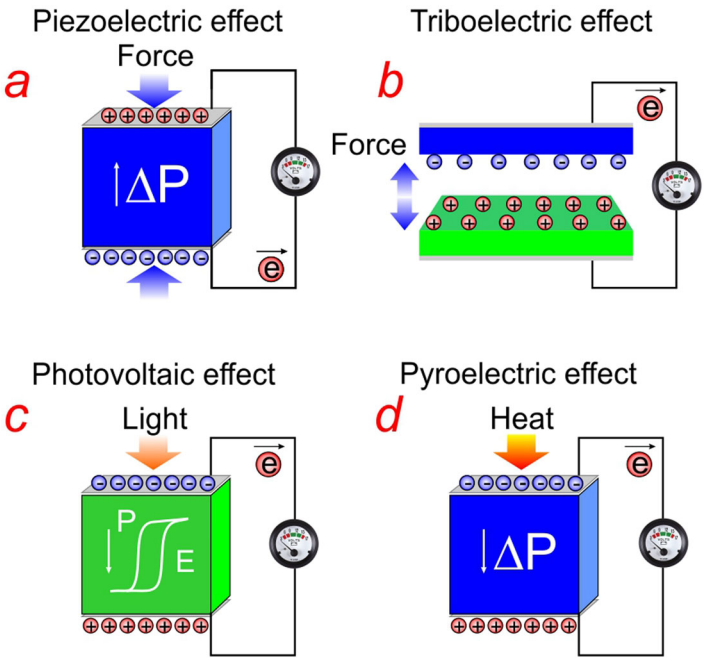

Figure 2. Schematic illustration of energy harvesters based on (*a*) the piezoelectric effect, (*b*) the triboelectric effect, (*c*) the pyroelectric effect, and (*d*) the photovoltaic effect.

(Figure 2d). When light is incident upon a PV cell, electricity is generated through the light absorption by the semiconductor, excitation, hole/electron separation, and the transport of charges to the electrodes.

2.4. Pyroelectric Effect

Pyroelectric energy harvesting technology is based on the change in spontaneous polarization of certain anisotropic solids due to the temperature fluctuation (Figure 2c). By harvesting the waste thermal energy, pyroelectric nanogenerators have potential applications such as environmental monitoring and personal electronics [7].

Most of the alternative generators use one or two of the listed effects, but the device which we have developed is based on the simultaneous use of all of the above phenomena. This greatly increases the efficiency of this converter.

3. Experimental Setup

For measuring photovoltaic parameters, the studied samples of generators were illuminated using LED light sources produced by Thorlabs, namely M505L3 (505 nm), M660L4 (660 nm), M810L3 (810 nm), M940L3 (940 nm), and broadband MBB1L3 (470-850nm). We used a Thorlabs PM100 High Sensitivity Optical Power Meter to measure the illumination level with S120B (Si) sensor, which works in the wavelength range 400-1100nm and power range 50nW to 50mW. The output photovoltage level was fixed using OWON XDM 3041 digital multimeter.

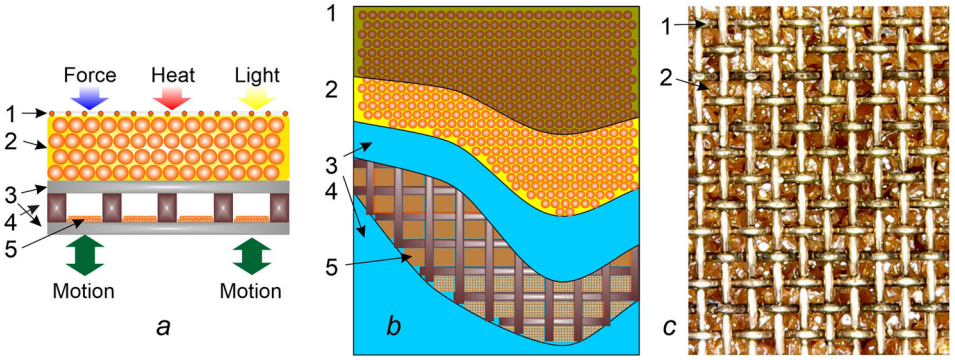

Figure 3. Sectional drawing of a multilayer transformer of deformation-motion-lighting and heating into electric current (*a,b*), and a photo of the enlarged area of the generator surface (*c*). 1 - translucent copper mesh electrode, 2 - composite based on $Sn_2P_2S_6$ powder, 3 - aluminum electrodes, 4 - rubber insulators, 5 - $Sn_2P_2S_6$ powder.

The generator capacitance and resistance were measured using a Goodwill LCR-819 meter. We used these parameters to estimate the time constant of the cell, which for a generator with an area of 1 cm^2 is approximately 1 s. This imposed a limitation on the method for determining the pyroelectric parameters of the converter. Instead of a dynamic method for measuring pyroelectric properties, a quasi-static method with a constant rate of temperature change had to be used. To measure the temperature, we used the LabVIEW controlled Measurement Computing USB-TEMP-AI data acquisition device. As a temperature sensor the PT100/1509A platinum thermistor of TDI Ltd. company (England) was applied. The temperature measurement accuracy was ±0.01 K. The heater power was changed using a Linear Programmable DC Power Supply OWON ODP3033.

The output voltage of the triboelectric generator was recorded using a Tektronix TDS-380 oscilloscope.

The measurements of hydrostatic voltage sensitivity were performed in an acoustic coupler (pistonphone). The loudspeaker was used as a source of acoustic excitation. The response of the sample was measured in the receiving mode at a frequency of 30 Hz. The absolute value of the sample sensitivity was evaluated by comparison with the response of the calibrated reference hydrophone, which was mounted in the coupler close to the sample. The specific piezoelectric voltage sensitivity g_h was calculated by dividing the value of the measured sensitivity by the thickness of the composite layer. The hydrostatic piezoelectric coefficient d_h is given by

$$d_h = g_h \cdot \varepsilon\varepsilon_0$$

4. Multi-Type Energy-Harvesting Device

We have developed a double layer converter of heating-deformation-lighting (upper layer) and motion/vibration (lower layer) into electricity. The design of the generator is shown in Figure 3. A composite or ceramic material (2) based on $Sn_2P_2S_6$ powder is applied to the base, for which a thin aluminum plate is used (3). It simultaneously

Table 1. Dielectric and electromechanical properties of $Sn_2P_2S_6$ single crystals, doped by 5 atomic % of Ge, $Sn_2P_2S_6$ +epoxy composite (with 84.7 vol % of $Sn_2P_2S_6$) and $Sn_2P_2S_6$ ceramics [2,7,9] at the room temperature.

	ε_{ii}	$d_h \cdot 10^{12}$ C/N	$g_h \cdot 10^3$ Vm/N	$d_h \cdot g_h \cdot 10^{15}$ m^2/N	Tc °C
$Sn_2P_2S_6$	280	320	145	46400	65
$Sn_2P_2S_6$ + 0.05Ge	220	365	187	68255	88
Ceramic $Sn_2P_2S_6$	120	85	80	6800	77
Composite $Sn_2P_2S_6$ Epoxy	40	55	155	8530	65
PZT Ceramics	600	200	50	10000	

serves as a mechanical base, one of the electrodes of the multi-type transducer, and another one of the plates of the triboelectric nanogenerator (TENG) transducer.

A thin copper mesh was used as a translucent electrode (1) with 50 × 50 µm holes. The advantages of a copper grid in comparison with a solid semitransparent electrode (for example SnO) are that the holes in the grid simultaneously serve as stabilizing and orienting elements for the $Sn_2P_2S_6$ crystal particles, and also has 3-4 orders of magnitude less resistance compared to SnO.

Thus, the first, top layer of the generator, which converts heat, light and deformation into electricity, consists of elements 1-3 and the second, lower layer of the generator, which converts motion and vibration into electricity, consists of elements 3-5, Figure 3a.

A grid of rubber insulators (4) is glued to the underside of the aluminum base electrode, which forms the elementary cells of TENG. The obtained cells of the triboelectric nanogenerator are 20% filled with $Sn_2P_2S_6$ powder (5), with a particle size of 70-80 µm.

During vibrations or movement, these particles rub against each other, forming a charge on the surface of the particles due to the piezoelectric effect as well as to the electrodes, accumulating and transferring the charge due to the triboelectric effect. This combination creates a 180 V potential between the electrodes. A similar principle of operation of a triboelectric nanogenerator was first described in the work [8].

A grid of rubber partitions insulates one cell from another, which creates the effect of parallel connection of a large number of elementary generator cells (to increase the output current) and preventing the flowing of the active substance from one cell to another.

Aluminum was not chosen as an electrode by chance but based on its position in the triboelectric table [9]. To increase the efficiency of the triboelectric nanogenerator and improve adhesion when applying the composite layer, the aluminum plate is microstructured by etching.

4.1. $Sn_2P_2S_6$ Ferroelectric Based Active Layer

The upper composite layer based on $Sn_2P_2S_6$ microcrystals provides the transformation of deformation/compression (due to the piezoelectric effect [10]), lighting (due to the photovoltaic effect [11]), and temperature change (due to the pyroelectric effect [12]) to electricity. This ferroelectric semiconductor has several unique parameters (Table 1). As shown earlier, to increase the operating temperature range $Sn_2P_2S_6$ single crystals must be doped with germanium which increases the phase transition temperature by 20 degrees without affecting its electrophysical parameters. As we can see in Table 1,

composites and ceramics based on crushed single crystals also have good piezoelectric and pyroelectric characteristics.

To create ceramics based on $Sn_2P_2S_6$ sintering of ground polycrystals at a temperature of 500°C is used [10].

A composite based on $Sn_2P_2S_6$ can be obtained by mixing sorted (by multiple sieving first through a sieve with a mesh size of 80 microns and then 71 microns, which guarantees particles in the range of 70-80 microns) microcrystals with epoxy resin or acrylic dissolved in dichloroethane. To increase the density of the obtained material it is advisable to carry out the sedimentation of the composite on a pre-prepared aluminum substrate in a centrifuge, with a high voltage applied between the substrate and the composite solution. This allows us to orient and polarize $Sn_2P_2S_6$ microcrystals during the hardening of the composite. Centrifuge compaction also improves the adhesion of the copper mesh and ferroelectric crystallite particles. After complete hardening of the mixture, the "extra layer" (which rises above the copper mesh) of acrylic or epoxy is mechanically sanded. If we put a flat aluminum plate (0.5 mm thick) in the centrifuge basket, which serves as the base for our transducer during centrifugation, it slightly deforms, but the radius of curvature of the centrifuge basket is 40 cm, and the sample is 2 cm wide. In this case, the radius of curvature of the transducer is less than 1 mm, and after removing the sample from the centrifuge, it straightens quite easily. After this procedure, the particles of the ferroelectric powder will be slightly deformed, which improves the contact of the copper mesh with $Sn_2P_2S_6$ microcrystallites.

The data of [7] reveal that the hydrostatic voltage sensitivity $g_h = d_h/\varepsilon\varepsilon_0$, (where d_h is a hydrostatic piezoelectric coefficient and ε is the dielectric constant) is enhanced in modified crystals compared to pure $Sn_2P_2S_6$. At the room temperature $\gamma = 7.5 \cdot 10^{-8}$ C/cm^{2}K and $\gamma = 6.2 \cdot 10^{-8}$ C/cm^{2}K for pure and doped $Sn_2P_2S_6$, respectively. A slight decrease in γ for Ge-doped crystal around the room temperature is obviously connected with the decrease in the temperature dependence of spontaneous polarization. This is believed to be related to the shift of T_c to higher temperatures.

4.2. Triboelectric Generator Cells

The cells of a triboelectric generator with a volume of 0.125 cm^3 (Figure 3, elements 3,4,5) per 1/3 were filled with a polyvinylidene fluoride powder, PZT piezoceramics, and then with ferroelectric $Sn_2P_2S_6$ micro crystallites 70-100 μm in size. The minimal size is limited by the ferroelectric parameters of the particles. Aluminum plates (3) were used as electrodes.

Our studies have shown that the efficiency of a triboelectric generator using the internal friction of the powder as the active substance depends significantly on the type of active material used. As we can see in Figure 4c. the amplitude of the output voltage is the largest in the case of ferroelectric microcrystals of the $Sn_2P_2S_6$ and exceeds the corresponding values for PVDF and piezoceramics by 4 times (16 V compared to 4 V for PVDF and piezoceramics). This is most likely due to the more efficient accumulation of charge on the surface of $Sn_2P_2S_6$ microparticles, and the additional charge that is formed on the surface of the grains due to the piezoelectric effect. With the optimal selection of the load resistance, the output voltage of the generator increases by 10

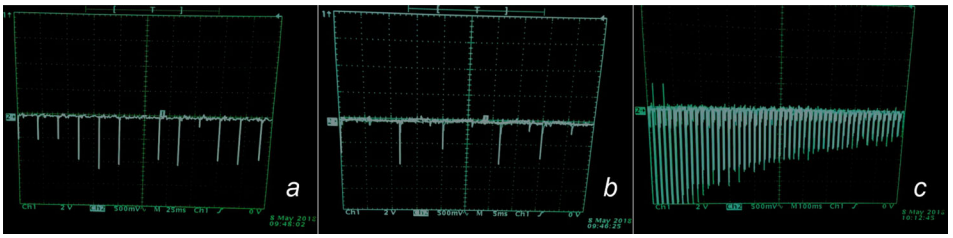

Figure 4. Oscillograms of the output voltage of a triboelectric nanogenerator using the internal friction of the powder as the active substance. (a) - polyvinylidene fluoride, (b) – PZT piezoceramics, (c) - $Sn_2P_2S_6$ microcrystals.

times. A load of 1 MOм allows obtaining an output voltage of 160 V. The oscillograms in the figure were taken with a 1/10 voltage divider to protect the input circuits of the oscilloscope. The measurements were carried out on a vibrating table with an oscillation amplitude of 10 mm and a frequency of 40-100 Hz.

As we can see on Figure 4c, the output amplitude of the generator decreases quite rapidly, due to the formation of a locking layer on the surface of the aluminum electrodes.

The liquid-like behavior of the powder removes the constraints on the geometric design of the generator cells. It is possible to create generator cells with different shapes and sizes (square, such as honeycombs, round). The distance between the electrodes (layer thickness) is limited only by the amplitude of oscillations. We have proposed to divide the working volume into a set of smaller cells. Finally, it provides an additional opportunity to increase the output voltage and current due to the parallel and/or series connection of the cells and prevents the "flow" of the working substance in the layer in one direction or another.

Stabilization of the generator cell parameters requires further research and can be implemented by strengthening the micro crystallites of the active substance, replacing them with composite materials, or using another type of oxide ferroelectric.

5. Experimental Data

For research, we have prepared many samples with different particle sizes and the ratio of the amount of glue and microparticles. The highest efficiency of the converter developed by us was obtained with a particle size of 70-100 microns. Reducing the particle size to less than 50 microns reduced very dramatically the efficiency of the generator. Larger particles are technologically problematic due to the orientation of such particles during the solidification of the composite. The use of a copper mesh is much more preferable than a transparent film with an evaporated semitransparent electrode since "excess" glue penetrates through the mesh holes during hardening.

For measurements, we used samples with physical dimensions $1 \times 1\,cm^2$. This size simplifies the estimation of the generator parameters.

As we can see in Figure 5, at an illumination power of approximately 20 mW at almost all wavelengths, the dependence of the output voltage on the intensity reaches saturation. An exception is the wavelength of 810 nm. At the same wavelength, the maximum output voltage is observed. This behavior can be explained both by the depth of

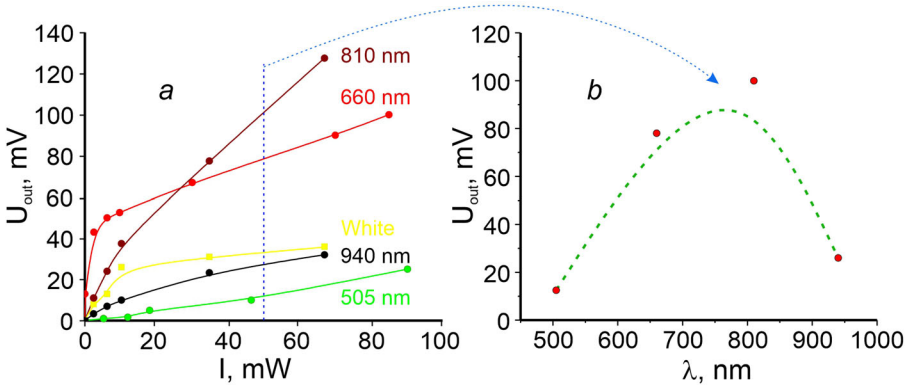

Figure 5. Dependence of the generator output voltage on the lighting power at different wavelengths (a) and on the wavelength (b) at a fixed lighting intensity (50 mW)..

radiation penetration into the crystal and by the manifestation of the pyroelectric contribution to the output voltage due to heating. The pyroelectric response in $Sn_2P_2S_6$ crystals is greater than the output voltage due to the photovoltaic effect. A significant drop in the output voltage with a further increase in wavelength, as seen in graph 2 at 940 nm, is most likely due to the absorption of long-wave radiation by the epoxy resin. The photovoltaic effect in these crystals is the smallest in comparison with the pyroelectric, piezoelectric, and triboelectric effects; however, the existence of such a contribution makes the use of ferroelectrics an interesting active material for combined alternative power sources. The maximum output voltage due to the lighting of our generator is 0.1 V, however, when such cells are connected in series on an area of 10×10 cm, we can get an output voltage of 10 V at a current of 1 μA. This provides an output power of 10 μW, which, of course, is not very much, but since this is just an additional output power to the pyroelectric, piezoelectric, and triboelectric response, in total we get a generator that can provide power to the Maxim MAXREFDES100# health sensor platform device from sunlight, body heating, human movement or vibrations.

6. Energy Harvesting Power Supply

To connect the designed generator to load, it is advisable to use one of the specialized energy harvesting integrated circuits for example LTC3330 of the Analog Devices Company.

The Dual Input, Single Output DC/DCs with Input Prioritizer IC LTC®3330 integrates a high voltage energy harvesting power supply plus a DC/DC converter powered by a primary cell battery to create a single output supply for alternative energy applications. The energy harvesting power supply, consisting of an integrated full-wave bridge rectifier and a high voltage buck converter, harvests energy from piezoelectric, solar, or magnetic sources. The primary cell input powers a buck-boost converter capable of operation down to 1.8 V at its input. Either DC/DC converter can deliver energy to a single output. The buck operates when harvested energy is available, reducing the quiescent current draw on the battery to essentially zero, thereby extending the life of the battery. The buck-boost powers VOUT only when harvested energy goes away [13].

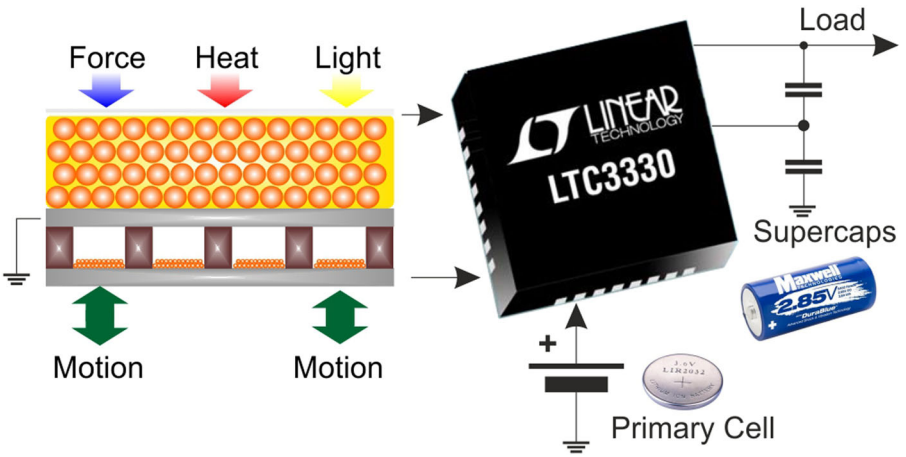

Figure 6. Multi-type energy-harvesting device connection option using LTC3330 chip.

A low noise LDO post regulator and a supercapacitor balancer are also integrated, accommodating a wide range of output storage configurations.

The use of two independent inputs allows us to connect a composite-based heating-compressing-lighting converter to one of the inputs of LTC3330, and a network of parallel-connected triboelectric nanogenerators to the second input of it (Figure 6).

7. Conclusions

Using a composite material based on a $Sn_2P_2S_6$ ferroelectric powder we have presented a multi-type energy-harvesting device for converting lighting-heating-motion and deformation to electricity. The estimated power of our multilayer converter is approximately 100 W/m^2 with an output voltage of 3.3 V (due to the used electronics and can easily be changed). The power output, of course, is a function of amplitude and frequency of vibrations and deformation as well as intensity of lighting and heating.

We have studied the photovoltaic properties of a generator based on a composite of $Sn_2P_2S_6$. At the wavelength of 810 nm, the maximum output voltage 0.1 V is observed, however, when such cells are connected in series on an area of 10×10 cm, we can get an output voltage of 10 V at a current of 1 μA.

The experimental sample was created for the autonomous energy supply of firefighter equipment (AR assisted health state telemetry system based on Maxim MAXREFDES100# health sensor platform), where powering of equipment is extremely important.

References

1. Y. Bai *et al.*, Ferroelectric, pyroelectric, and piezoelectric properties of a photovoltaic perovskite oxide, *Appl. Phys. Lett.* 110 (6), 063903 (2017). DOI: 10.1063/1.4974735.
2. M. M. Maior, I. P. Prits, and Y. M. Vysochanskii, Piezoelectric composite with high hydrostatic piezoelectric sensitivity, *Ferroelectrics* 266 (1), 247 (2002). DOI: 10.1080/00150190211449.
3. Y. M. Vysochanskii *et al.*, *Phase Transitions in Ferroelectric Phosphorous Chalcogenide Crystals* (Vilnius University Publishing House, Lithuania, 2006), p. 453.

4. A. Gritsenko, V. Nikiforov, and T. Shchegolev, Status and prospects of development of piezoelectric generators, *Compon. Technol*. 9, 63–68 (2012).
5. Z. L. Wang, Triboelectric nanogenerators as new energy technology and self-powered sensors - principles, problems and perspectives, *Faraday Discuss*. 176, 447 (2014). DOI: 10.1039/C4FD00159A.
6. A. V. Solnyshkin *et al.*, Photovoltaic and photoelectric response of $Sn_2P_2S_6$ ferroelectric films, *J. Adv. Dielectr*. 09 (01), 1950003 (2019). DOI: 10.1142/S2010135X19500036.
7. M. M. Maior *et al.*, Effect of Germanium doping on pyroelectric and piezoelectric properties of Sn(2)P(2)S(6) single crystal, *IEEE Trans. Ultrason. Ferroelectr. Freq. Control.* 47 (4), 877 (2000). DOI: 10.1109/58.852069.
8. D. Kim *et al.*, Triboelectric nanogenerator based on the internal motion of powder with a package structure design, *ACS Nano*. 10 (1), 1017 (2016). DOI: 10.1021/ACSNANO.5B06329.
9. O. Molnar, V. Gerasimov, and I. P. Kurytnik, Triboelectricity and construction of power generators based on it, *Przeglad Elektrotechniczny* 1, 167 (2018). DOI: 10.15199/48.2018.01.41.
10. M. M. Maior *et al.*, Piezoelectric properties of $Sn_2P_2S_6$ ceramics, *Ferroelectr. Lett.* 33 (3–4), 31 (2006). DOI: 10.1080/07315170600870618.
11. Y. W. Cho, S. K. Choi, and Y. M. Vysochanskii, Photovoltaic effect of $Sn_2P_2S_6$ ferroelectric crystal and ceramics, *J. Mater. Res.* 16 (11), 3317 (2001). DOI: 10.1557/JMR.2001.0456.
12. S. L. Bravina *et al.*, Pyroelectric properties of crystals $Sn_2P_2S_6$, *Izv. AN USSR. Neorg. Mater*. 23 (5), 733 (1987).
13. Linear Technology LTC3330 - Nanopower Buck-Boost DC/DC with Energy Harvesting Battery Life Extender, Datasheet Rev. C 32 (2013).